

Outage Analysis of Uplink IRS-Assisted NOMA under Elements Splitting

Bashar Tahir, Stefan Schwarz, and Markus Rupp

Institute of Telecommunications, Technische Universität Wien, Vienna, Austria

Abstract—In this paper, we investigate the outage performance of an intelligent reflecting surface (IRS)-assisted non-orthogonal multiple access (NOMA) uplink, in which a group of the surface reflecting elements are configured to boost the signal of one of the user equipments (UEs), while the remaining elements are used to boost the other UE. By approximating the received powers as Gamma random variables, tractable expressions for the outage probability under NOMA interference cancellation are obtained. We evaluate the outage over different splits of the elements and varying pathloss differences between the two UEs. The analysis shows that for small pathloss differences, the split should be chosen such that most of the IRS elements are configured to boost the stronger UE, while for large pathloss differences, it is more beneficial to boost the weaker UE. Finally, we investigate a robust selection of the elements' split under the criterion of minimizing the maximum outage between the two UEs.

I. INTRODUCTION

Intelligent reflecting surfaces (IRSs), also known as reconfigurable intelligent surfaces (RISs), have been identified as a promising technology to enhance the spectral and energy efficiency of beyond fifth-generation (B5G) wireless systems [1], [2]. Those surfaces consist of a large number of low-cost reconfigurable elements whose electromagnetic response to impinging/incident waves can be modified. Phase adjustment of the waves across the different elements allows the surface to perform passive beamforming, which is beneficial in the context of extending the coverage area, focusing the energy towards a certain user equipment (UE), reducing interference, and more [3], [4].

Another technology that has gained interest over the past couple of years is non-orthogonal multiple access (NOMA). With NOMA, the UEs can contest the same time-frequency resources in a non-orthogonal manner, which may lead to a higher spectral efficiency, lower access latency, improved user fairness, etc [5], [6]. The combination of NOMA with IRSs has gained attention recently, with many works showing potential gains in terms of energy efficiency, sum-rate, and outage performance [7]–[11]. An important aspect is how to configure the elements of the surface. In some works, the phase shifts across the different elements are set jointly according to a certain design criterion [8], [9], [12], such as maximizing the sum-rate. Other works consider the case where the entire surface is used to boost one of the NOMA UEs [7], [10].

Bashar Tahir and Stefan Schwarz are with the Christian Doppler Laboratory for Dependable Wireless Connectivity for the Society in Motion. The financial support by the Austrian Federal Ministry for Digital and Economic Affairs and the National Foundation for Research, Technology and Development is gratefully acknowledged.

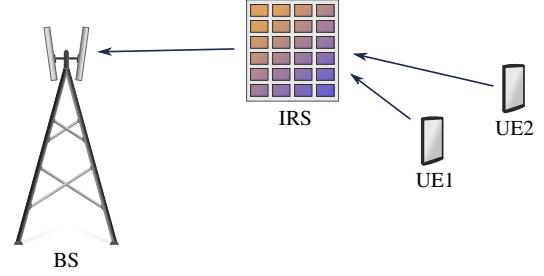


Fig. 1: The uplink IRS-assisted NOMA setup.

We consider in this paper an IRS-assisted NOMA uplink, in which the elements of the IRS are split between the two NOMA UEs, i.e., part of the surface is used to coherently combine the signal of the first UE, while the other part is used to coherently combine the signal of the second one. We assume the communication to take place primarily through the surface, e.g., due to blockage of the direct links to the base station (BS). All the links are assumed to undergo Nakagami- m fading, allowing to flexibly capture line-of-sight (LOS) and non-line-of-sight (NLOS) propagation conditions. We analyze the outage probability under NOMA interference cancellation (IC) for different splits of the elements and pathloss differences between the UEs. To obtain tractable expressions, we approximate the received powers of the UEs as Gamma random variables (RVs) in a fashion similar to [13], [14] via second-order moments matching. We finally analyze an outage-robust selection of the elements' split between the two UEs and discuss its impact on the performance limits of such a system.

II. SYSTEM MODEL

We consider a single-antenna two-UE NOMA uplink assisted by an N -elements IRS, as shown in Figure 1. At the BS, the received signal is given by

$$r = \sum_{i=1}^2 \sqrt{\ell_{\text{BS}} \ell_{h_i} P_i} \mathbf{h}_{\text{BS}}^T \mathbf{\Phi} \mathbf{h}_i x_i + w, \quad (1)$$

where $\mathbf{h}_{\text{BS}} \in \mathbb{C}^N$, and $\mathbf{h}_i \in \mathbb{C}^N$ are the small-scale fading coefficients of the BS-IRS and IRS-UE links, respectively. The parameters ℓ_{BS} and ℓ_{h_i} are the corresponding pathlosses, P_i and x_i are the transmit power and signal of the i^{th} -UE, and w is the zero-mean Gaussian noise with power P_w . The phase-shift matrix $\mathbf{\Phi} \in \mathbb{C}^{N \times N}$ is defined as

$$\mathbf{\Phi} = \text{diag}(e^{j\phi_1}, e^{j\phi_2}, \dots, e^{j\phi_N}), \quad (2)$$

where ϕ_n is the phase-shift applied at the n^{th} -element of the IRS. Note that the IRS term can be written equivalently as

$$\mathbf{h}_{\text{BS}}^T \Phi \mathbf{h}_i = \sum_{n=1}^N e^{j\phi_n} \mathbf{h}_{\text{BS},n} \mathbf{h}_{i,n}, \quad (3)$$

where $\mathbf{h}_{\text{BS},n}$ and $\mathbf{h}_{i,n}$ are the n^{th} -elements of \mathbf{h}_{BS} and \mathbf{h}_i , respectively. To be flexible in terms of modeling LOS and NLOS propagation conditions, the links are assumed to undergo Nakagami- m fading, i.e.,

$$\begin{aligned} |\mathbf{h}_{\text{BS},n}| &\sim \text{Nakagami}(m_{\text{BS}}, 1), \\ |\mathbf{h}_{i,n}| &\sim \text{Nakagami}(m_{h_i}, 1), \end{aligned} \quad (4)$$

where m_{BS} and m_{h_i} are the corresponding distribution parameters.

In this work, we consider the case where the elements of the IRS is split between the two UEs, i.e., a total of N_1 elements are configured to coherently combine the signal of UE1, while $N_2 = N - N_1$ elements are configured for UE2. The phases are then set to

$$\phi_n = -\arg(\mathbf{h}_{\text{BS},n} \mathbf{h}_{i,n}), \quad n \in \mathcal{C}_i, \quad (5)$$

where \mathcal{C}_i is the set of elements that are configured to boost the i^{th} -UE. Therefore, the IRS term can be written as

$$\mathbf{h}_{\text{BS}}^T \Phi \mathbf{h}_i = \underbrace{\sum_{n \in \mathcal{C}_i} |\mathbf{h}_{\text{BS},n}| |\mathbf{h}_{i,n}|}_{\text{coherently combined part of the } i^{\text{th}}\text{-UE}} + \underbrace{\sum_{n \in \bar{\mathcal{C}}_i} e^{j\phi_n} \mathbf{h}_{\text{BS},n} \mathbf{h}_{i,n}}_{\text{randomly combined part of the } i^{\text{th}}\text{-UE}}, \quad (6)$$

where the complement set $\bar{\mathcal{C}}_i$ is the set of elements that are not configured for the i^{th} -UE, and thus will result in a random combining of its phases. Note that $\mathcal{C}_1 = \bar{\mathcal{C}}_2$, i.e., the part that will coherently combine the signal of one of the UEs, will randomly combine the signal of the other one. This is under the assumption that the channels of the two UEs are uncorrelated.

Since we apply the Gamma moment matching often in this work, we state how it is performed in the following lemma.

Lemma 1. Let X be a non-negative RV with first and second moments given by $\mu_X = \mathbb{E}\{X\}$ and $\mu_X^{(2)} = \mathbb{E}\{X^2\}$, respectively. The Gamma RV $Y \sim \Gamma(k, \theta)$ with the same first and second moments has shape k and scale θ parameters

$$k = \frac{\mu_X^2}{\mu_X^{(2)} - \mu_X^2}, \quad \theta = \frac{\mu_X^{(2)} - \mu_X^2}{\mu_X}.$$

Additionally, Gamma RVs satisfy the scaling property, in the sense that if $Y \sim \Gamma(k, \theta)$, then $cY \sim \Gamma(k, c\theta)$.

III. OUTAGE ANALYSIS

Evaluating metrics such as the NOMA outage probability requires an access to the statistics of the channel output power, preferably the full distribution. As can be seen in (6), that is no easy task. Therefore, we resort to approximations. Our approach here is to approximate the received powers of the NOMA UEs as Gamma RVs. On the one hand, the Gamma

distribution can accurately model the power of many fading distributions, and on the other hand, it allows for tractable expressions when evaluating the outage, as we will see later.

A. Statistics of the Received Power

Let Z_i be the channel power of the i^{th} -UE, i.e.,

$$Z_i = \ell_{\text{BS}} \ell_{h_i} \left| \sum_{n \in \mathcal{C}_i} |\mathbf{h}_{\text{BS},n}| |\mathbf{h}_{i,n}| + \sum_{n \in \bar{\mathcal{C}}_i} e^{j\phi_n} \mathbf{h}_{\text{BS},n} \mathbf{h}_{i,n} \right|^2. \quad (7)$$

Our goal here is to approximate Z_i as a Gamma RV via second-order moments matching, which requires an access to its first two moments. To simplify matters, we first address the statistics of the two sum terms inside.

Lemma 2. For the two sum terms in (7) given by

$$\begin{aligned} S_{\mathcal{C}_i} &= \sum_{n \in \mathcal{C}_i} |\mathbf{h}_{\text{BS},n}| |\mathbf{h}_{i,n}|, \\ S_{\bar{\mathcal{C}}_i} &= \sum_{n \in \bar{\mathcal{C}}_i} e^{j\phi_n} \mathbf{h}_{\text{BS},n} \mathbf{h}_{i,n}, \end{aligned}$$

their distributions are approximated as

$$\begin{aligned} S_{\mathcal{C}_i} &\overset{\text{approx}}{\sim} \Gamma\left(N_i \frac{\mu_i^2}{1 - \mu_i^2}, \frac{1 - \mu_i^2}{\mu_i}\right), \\ S_{\bar{\mathcal{C}}_i} &\overset{\text{approx}}{\sim} \mathcal{CN}(0, N - N_i), \end{aligned}$$

with

$$\mu_i = \mathbb{E}\{|\mathbf{h}_{\text{BS},n}| |\mathbf{h}_{i,n}|\} = \frac{\Gamma(m_{\text{BS}} + \frac{1}{2}) \Gamma(m_{h_i} + \frac{1}{2})}{\Gamma(m_{\text{BS}}) \Gamma(m_{h_i}) (m_{\text{BS}} m_{h_i})^{1/2}},$$

being the mean of the product of two independent Nakagami RVs.

Proof. We follow a similar approach as in [13]. The first term is a sum of N_i i.i.d. positive RVs that can be well approximated by a Gamma RV via moments matching (Lemma 1), requiring access only to the mean of the composite channel (μ_i). For the second term, it is a sum of $N - N_i$ complex-valued i.i.d. RVs, which are approximated by a zero-mean complex Gaussian. \square

The channel power now can be compactly written as

$$Z_i = \ell_{\text{BS}} \ell_{h_i} |S_{\mathcal{C}_i} + S_{\bar{\mathcal{C}}_i}|^2, \quad (8)$$

with the first two moments given by the following lemma.

Lemma 3. The first two moments of the channel power under elements splitting are given by

$$\begin{aligned} \mu_{Z_i} &= \ell_{\text{BS}} \ell_{h_i} \left(\mu_{S_{\mathcal{C}_i}}^{(2)} + \mu_{|S_{\bar{\mathcal{C}}_i}|}^{(2)} \right), \\ \mu_{Z_i}^{(2)} &= (\ell_{\text{BS}} \ell_{h_i})^2 \left(\mu_{S_{\mathcal{C}_i}}^{(4)} + \mu_{|S_{\bar{\mathcal{C}}_i}|}^{(4)} + 4 \mu_{S_{\mathcal{C}_i}}^{(2)} \mu_{|S_{\bar{\mathcal{C}}_i}|}^{(2)} \right), \end{aligned}$$

where

$$\begin{aligned} \mu_{S_{\mathcal{C}_i}}^{(p)} &= \frac{\Gamma\left(N_i \frac{\mu_i^2}{1 - \mu_i^2} + p\right) \left(\frac{1 - \mu_i^2}{\mu_i}\right)^p}{\Gamma\left(N_i \frac{\mu_i^2}{1 - \mu_i^2}\right)}, \\ \mu_{|S_{\bar{\mathcal{C}}_i}|}^{(p)} &= \Gamma\left(1 + \frac{p}{2}\right) (N - N_i)^{p/2}. \end{aligned}$$

Proof. Expanding (8), we have

$$\mu_{Z_i} = \ell_{\text{BS}} \ell_{h_i} \mathbb{E}\{S_{\bar{C}_i}^2 + |S_{\bar{C}_i}|^2 + 2S_{\bar{C}_i} \Re\{S_{\bar{C}_i}\}\}.$$

We make the assumption here that the phase of $S_{\bar{C}_i}$ is zero-mean symmetric. This is valid since it results from an out-of-phase summation of the terms. Therefore, its real part will be zero-mean as well, leading to $\mathbb{E}\{S_{\bar{C}_i} \Re\{S_{\bar{C}_i}\}\} = \mathbb{E}\{S_{\bar{C}_i}\} \mathbb{E}\{\Re\{S_{\bar{C}_i}\}\} = 0$, giving the final result. We proceed in a similar manner for $\mu_{Z_i}^{(2)}$. After the expansion we get

$$\mu_{Z_i}^{(2)} = (\ell_{\text{BS}} \ell_{h_i})^2 \mathbb{E}\{S_{\bar{C}_i}^4 + |S_{\bar{C}_i}|^4 + 2S_{\bar{C}_i}^2 |S_{\bar{C}_i}|^2 + 4S_{\bar{C}_i}^3 \Re\{S_{\bar{C}_i}\} + 4S_{\bar{C}_i} |S_{\bar{C}_i}|^2 \Re\{S_{\bar{C}_i}\} + 4S_{\bar{C}_i}^2 \Re\{S_{\bar{C}_i}\}^2\}.$$

Following the assumptions of independence and zero-mean symmetry, we have

$$\mathbb{E}\{S_{\bar{C}_i}^3 \Re\{S_{\bar{C}_i}\}\} = \mathbb{E}\{S_{\bar{C}_i}^3\} \mathbb{E}\{\Re\{S_{\bar{C}_i}\}\} = 0,$$

and

$$\begin{aligned} \mathbb{E}\{S_{\bar{C}_i} |S_{\bar{C}_i}|^2 \Re\{S_{\bar{C}_i}\}\} &= \mathbb{E}\{S_{\bar{C}_i}\} \mathbb{E}\{|S_{\bar{C}_i}|^2 \Re\{S_{\bar{C}_i}\}\} \\ &= \mathbb{E}\{S_{\bar{C}_i}\} \mathbb{E}\{\Re\{S_{\bar{C}_i}\}^3\} \\ &\quad + \Im\{S_{\bar{C}_i}\} \mathbb{E}\{S_{\bar{C}_i}\} \\ &= 0, \end{aligned}$$

where the final result follows from the fact that the third moment is zero as well (due to symmetry), and independence between the real and imaginary parts. For the last term, we assume that the power is split equally across the real and imaginary parts, and therefore

$$\mathbb{E}\{S_{\bar{C}_i}^2 \Re\{S_{\bar{C}_i}\}^2\} = \mathbb{E}\{S_{\bar{C}_i}^2\} \mathbb{E}\{|S_{\bar{C}_i}|^2\} / 2.$$

We get the final results by collecting the terms back and substituting the moments of Gamma and Rayleigh (magnitude of Gaussian) RVs. \square

After scaling with the transmit power, the received power of the i^{th} -UE is given by

$$Z_i P_i \stackrel{\text{approx}}{\sim} \Gamma(k_i, P_i \theta_i), \quad (9)$$

where k_i and θ_i are the Gamma parameters matched to the moments in Lemma 3.

B. Outage Probability under Interference Cancellation

Before applying IC, the signal-to-interference-plus-noise ratio (SINR) outage of the i^{th} -UE under the presence of interference from the j^{th} -UE is defined as

$$p_{\text{out}}^{(i)} = \mathbb{P}\left\{\frac{Z_i P_i}{Z_j P_j + P_w} \leq \epsilon\right\}, \quad (10)$$

where ϵ is the outage threshold. Under the Gamma approximation, this can be calculated as [13]

$$p_{\text{out}}^{(i)} \approx I\left(\frac{\epsilon \hat{\theta}_j}{\hat{\theta}_i + \epsilon \hat{\theta}_j}; \hat{k}_i, \hat{k}_j\right),$$

Parameter	Value
#IRS elements	$N = 32$
Transmit powers	$P_1 = P_2 = 30$ dBm
Nakagami parameters	$m_{\text{BS}} = 6$ $m_{h_1} = 3, m_{h_2} = 1.5$
Pathlosses	$\ell_{\text{BS}} = -65$ dB $\ell_{h_1} = -70$ dB, ℓ_{h_2} is variable
Noise power	$P_w = -110$ dBm

TABLE I: Scenario parameters.

where $I(\cdot; \cdot, \cdot)$ is the regularized incomplete beta function, and

$$\begin{aligned} \hat{k}_i &= k_i, & \hat{\theta}_i &= \theta_i P_i, \\ \hat{k}_j &= \frac{(k_j \theta_j P_j + P_w)^2}{k_j (\theta_j P_j)^2}, & \hat{\theta}_j &= \frac{k_j (\theta_j P_j)^2}{k_j \theta_j P_j + P_w}. \end{aligned} \quad (11)$$

If the interference is later removed via IC, only the noise remains; we define the signal-to-noise ratio (SNR) outage as

$$p_{\text{out, SNR}}^{(i)} = \mathbb{P}\left\{\frac{Z_i P_i}{P_w} \leq \epsilon\right\}, \quad (12)$$

which is simply the cumulative distribution function (CDF) of Z_i (Gamma RV) evaluated at $\epsilon P_w / P_i$. We consider here a parallel IC scheme, in which UE1, UE2, or both can be detected correctly at the first iteration if they are above the outage threshold. Whatever remains could be detected in the next iteration after IC in the presence of noise only. Following the path of successful detection for the i^{th} -UE, its outage probability under IC is given by [13]

$$p_{\text{out, IC}}^{(i)} \approx 1 - \min(p_{\text{succ}}^{(i)} + p_{\text{succ}}^{(j)} p_{\text{succ, SNR}}^{(i)}, p_{\text{succ, SNR}}^{(i)}), \quad (13)$$

where $p_{\text{succ}}^{(i)} = 1 - p_{\text{out}}^{(i)}$ and $p_{\text{succ, SNR}}^{(i)} = 1 - p_{\text{out, SNR}}^{(i)}$ are the corresponding success probabilities.

IV. ANALYSIS OF AN EXAMPLE SCENARIO

We consider a scenario where the communication between the NOMA UEs and the BS takes place through a 32-elements IRS, and evaluate the outage performance using (13). We assume the IRS to have a strong LOS connection to the BS, while the UEs have moderate LOS to the IRS, with UE1 having a stronger LOS than UE2. This is set by adjusting the corresponding Nakagami m parameters. The pathloss of UE1 is fixed to -70 dB, while for UE2, it varies. Without loss of generality, we assume that both UEs are transmitting with the same power, i.e., $P_1 = P_2$. In practice, the UEs might transmit with different powers; however, that does not affect the validity of our analysis here. It holds for any choice of P_1 and P_2 . The simulation parameters are summarized in Table I.

A. Impact of Elements Splitting

We define the split factor α as the percentage of elements that are allocated for the coherent combining of the signal of UE1. Given that N_1 elements are allocated to UE1, the split factor then is defined as

$$\alpha = N_1 / N, \quad (14)$$

and thus the number of elements allocated for UE2 is

$$N_2 = N - \lceil \alpha N \rceil. \quad (15)$$

When $\alpha = 1$, all the elements are allocated to UE1, while for $\alpha = 0$, all the elements are allocated to UE2, etc.

We investigate the outage performance over the split factor α for different outage thresholds. Figure 2a shows the performance when the UEs have the same pathloss, and therefore the average power gap between them is 0 dB (ignoring the surface processing). In that case, the outage probability for both UEs is minimized, if most of the elements are configured to boost one of the UEs. The reason for this is, when the split is close to 50%, then it is more likely that both UEs will be received with similar strength at the BS. This, in turn, makes the IC more difficult, since the UEs would suffer strong interference from each other. Therefore, when the pathloss difference between the two UEs is small, it makes sense to focus on boosting one of the UEs, such that the power gap between them increases, allowing the stronger UE to be detected correctly at the first IC iteration with high probability.

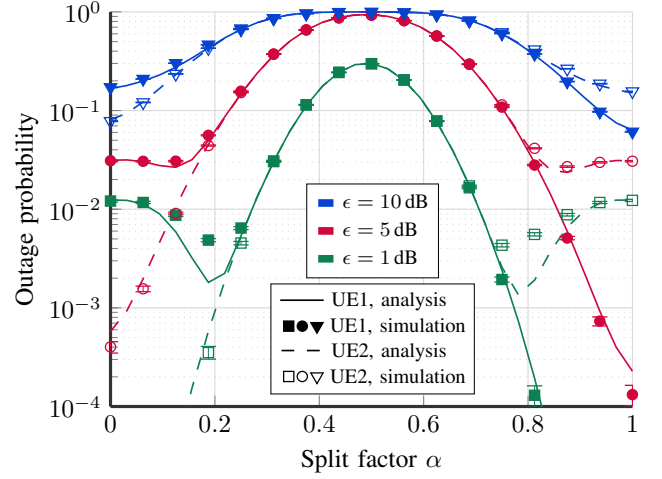
Figure 2b and Figure 2c show the outage performance when the pathloss of UE2 is 5 dB and 10 dB higher than UE1, respectively. We observe that as the gap increases, and at low outage thresholds, the split moves towards boosting UE2. In this case, the two UEs have a natural power gap due to the pathloss difference, and therefore the IRS can be used to enhance the performance of the weaker user (UE2). It can also be observed that as the gap increases, better performance is achieved for both UEs. This indicates that when it comes to NOMA user pairing, the BS should avoid pairing users with similar pathlosses. However, the weak UE should be strong enough such that after the combining at the surface, it is able to overcome the noise at the BS receiver. Regarding the accuracy of the analysis, we observe that the approximations hold well for the strong UE. As for the weak UE, and at low outage thresholds, a relatively large gap exists between analysis and simulation for some values of the split factor, suggesting that the Gamma approximation does not hold well under such splitting conditions.

B. Selection of the Split Factor

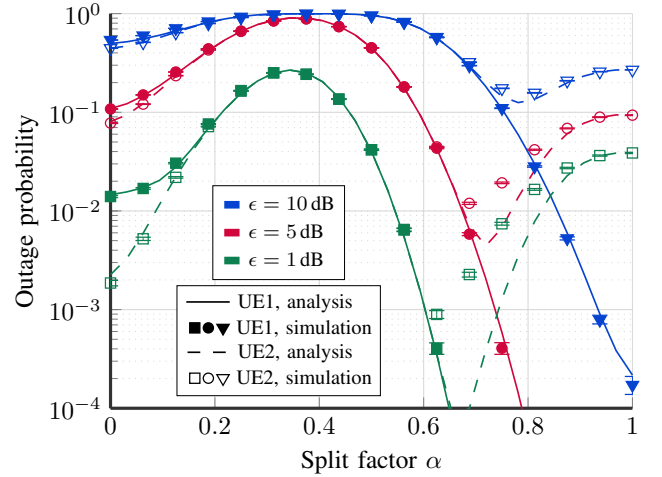
We consider the selection of the split factor α from a robust perspective. To ensure that boosting the performance of one UE does not come at the cost of degrading the performance of the other one, the split factor is chosen according to

$$\alpha_{\text{robust}} = \arg \min_{\alpha} \max_i p_{\text{out}, \text{IC}}^{(i)}. \quad (16)$$

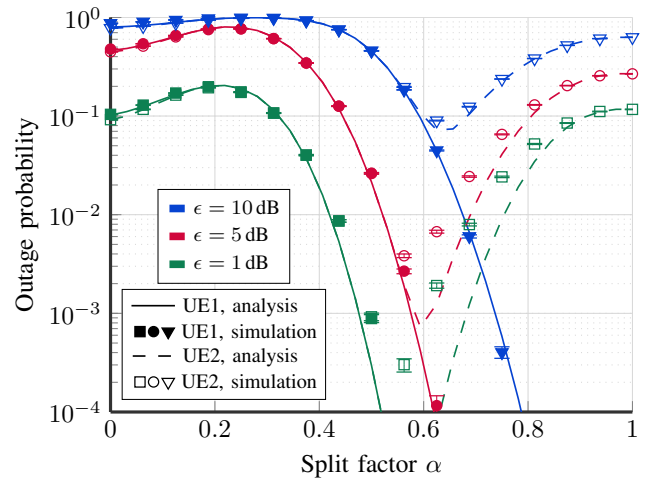
In Figure 2a to 2c, this would correspond to the points where the UE2 outage diverges from UE1 and starts saturating (on the right side). However, at high outage thresholds, it can be observed that the outage probability of UE2 is very high, no matter what split is applied. For that reason, we introduce the notion of a limiting threshold λ . If the weak UE outage probability is higher than λ , then the entire IRS is used to boost the strong UE, as allocating elements to the weak UE



(a) Equal pathloss case.



(b) UE2 5 dB weaker.



(c) UE2 10 dB weaker.

Fig. 2: Analysis of the outage probability vs. the split factor for different outage thresholds.

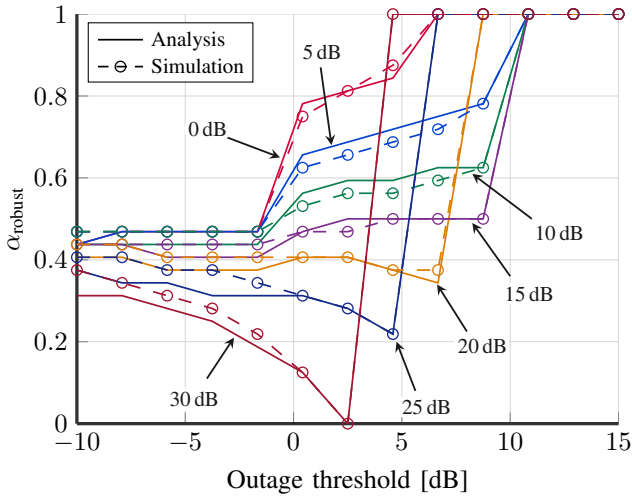


Fig. 3: Robust selection of the split factor for different pathloss gaps (search via analysis vs. exhaustive simulations).

would be a waste of the surface elements. Assuming UE2 is the weaker UE, (16) is modified as follows

$$\alpha_{\text{robust}} = \begin{cases} \arg \min_{\alpha} \max_i p_{\text{out}, \text{IC}}^{(i)}, & \text{if } p_{\text{out}, \text{IC}}^{(2)} < \lambda, \\ 1, & \text{otherwise.} \end{cases} \quad (17)$$

Although the analysis results shown in the previous subsection is not accurate at low outage thresholds, it can be seen that the robust point occurs almost at the same α for both analysis and simulation. This motivates the use of the analysis as a method to determine α_{robust} . Solving (17) in closed-form is difficult due to the complexity of the functions involved. We thus rely on performing a search for determining the optimal point. Recall that $\alpha = N_1/N$ with $N_1 = 1, 2, \dots, N$ (i.e., the maximum number of possibilities is N), meaning that the search can be performed quickly.

Figure 3 shows α_{robust} obtained by search through exhaustive simulations vs. analysis for different pathloss gaps between the two UEs. We observe that at low pathloss gaps, the split is chosen to boost UE1 (the stronger UE), since it improves the performance of the NOMA IC. As the pathloss of UE2 increases, the robust IRS strategy attempts to compensate for the high pathloss by allocating more elements to UE2. The sudden jumps to 1 are due to the limiting threshold, which is set to $\lambda = 10^{-1}$ here. This indicates that at those outage thresholds, the performance of UE2 is unacceptable anyway, that it is better to use the entire surface to boost UE1. Also, at low outage thresholds, we observe that a split close to 50% seems to be the robust selection, while at high outage thresholds, the selection across the different gaps can vary substantially. Note that at low outage thresholds, the outage probability is very low, which makes the simulation-based selection inaccurate, since it would require a huge number of simulation samples. This is the advantage of the analytical based approach, since it can predict the performance, even at very low outage probabilities.

V. CONCLUSION

In this work, we investigate the outage performance of a two-UEs IRS-assisted NOMA uplink, in which the elements of the surface are split between the two UEs. A Gamma approximation of the UEs received power is applied, allowing for tractable expressions of the outage under NOMA IC, while being able to capture LOS and NLOS propagation conditions. Our results show that when the pathloss difference between the NOMA UEs is small, then better outage performance is achieved if most of the surface elements are configured to boost the stronger UE. This further increases the power gap between the two UEs at the BS receiver, and thus improves the performance of IC at the first iteration. As the pathloss difference increases, then more elements should be allocated to boosting the weaker UE. In this case, a natural power gap exists between the UEs due to the pathloss difference, and therefore the split should be chosen to boost the performance of the weak UE, such that it is able to overcome the noise. At the end, we investigate a robust selection of the split factor based on minimizing the maximum outage between the two UEs, and show that such a split can be well predicted using our analysis.

REFERENCES

- [1] M. D. Renzo *et al.*, "Smart radio environments empowered by reconfigurable AI meta-surfaces: an idea whose time has come," *EURASIP Journal on Wireless Communications and Networking*, vol. 2019, no. 1, p. 129, May 2019.
- [2] Q. Wu and R. Zhang, "Intelligent Reflecting Surface Enhanced Wireless Network via Joint Active and Passive Beamforming," *IEEE Transactions on Wireless Communications*, vol. 18, no. 11, pp. 5394–5409, 2019.
- [3] —, "Towards Smart and Reconfigurable Environment: Intelligent Reflecting Surface Aided Wireless Network," *IEEE Communications Magazine*, vol. 58, no. 1, pp. 106–112, 2020.
- [4] E. Basar *et al.*, "Wireless Communications Through Reconfigurable Intelligent Surfaces," *IEEE Access*, vol. 7, pp. 116 753–116 773, 2019.
- [5] L. Dai *et al.*, "A Survey of Non-Orthogonal Multiple Access for 5G," *IEEE Communications Surveys Tutorials*, vol. 20, no. 3, pp. 2294–2323, 2018.
- [6] Z. Ding *et al.*, "Application of Non-Orthogonal Multiple Access in LTE and 5G Networks," *IEEE Communications Magazine*, vol. 55, no. 2, pp. 185–191, 2017.
- [7] Z. Ding and H. Vincent Poor, "A Simple Design of IRS-NOMA Transmission," *IEEE Communications Letters*, vol. 24, no. 5, pp. 1119–1123, 2020.
- [8] M. Fu, Y. Zhou, and Y. Shi, "Intelligent Reflecting Surface for Downlink Non-Orthogonal Multiple Access Networks," in *2019 IEEE Globecom Workshops (GC Wkshps)*, 2019, pp. 1–6.
- [9] G. Yang, X. Xu, and Y. Liang, "Intelligent Reflecting Surface Assisted Non-Orthogonal Multiple Access," in *2020 IEEE Wireless Communications and Networking Conference (WCNC)*, 2020, pp. 1–6.
- [10] Y. Cheng *et al.*, "Downlink and Uplink Intelligent Reflecting Surface Aided Networks: NOMA and OMA," *IEEE Transactions on Wireless Communications*, pp. 1–1, 2021.
- [11] Z. Ding, R. Schober, and H. V. Poor, "On the Impact of Phase Shifting Designs on IRS-NOMA," *IEEE Wireless Communications Letters*, vol. 9, no. 10, pp. 1596–1600, 2020.
- [12] M. Zeng *et al.*, "Sum Rate Maximization for IRS-assisted Uplink NOMA," *IEEE Communications Letters*, pp. 1–1, 2020.
- [13] B. Tahir, S. Schwarz, and M. Rupp, "Analysis of Uplink IRS-Assisted NOMA under Nakagami-m Fading via Moments Matching," *IEEE Wireless Communications Letters*, pp. 1–1, 2020.
- [14] J. Lyu and R. Zhang, "Spatial Throughput Characterization for Intelligent Reflecting Surface Aided Multiuser System," *IEEE Wireless Communications Letters*, vol. 9, no. 6, pp. 834–838, 2020.